13838 *Biochemistry* 1993, *32,* 13838-13843

Crystal Structure of d(CGCGAATTCGCG) Complexed with Propamidine, a Short-Chain Homologue of the Drug Pentamidine[†,‡]

Christine M. Nunn, Terence C. Jenkins, and Stephen Neidle*

Cancer Research Campaign Biomolecular Structure Unit, The Institute of Cancer Research, Sutton, Surrey SM2 5NG, U.K.

Received July 28, 1993; Revised Manuscript Received October 6, 1993[®]

ABSTRACT: The crystal structure of the complex between propamidine and the self-complementary DNA dodecamer d(CGCGAATTCGCG) duplex has been determined to a resolution of 2.1 Å and an *R*-factor of 17.4%. The propamidine binds to the DNA within the minor groove, with specific hydrogen-bonding interactions from the amidinium groups to the bases and sugar groups of the DNA, via a 4-base-pair binding site. A network of water molecules lies over the mouth of the minor groove. The structure provides a rationale for the superior DNA-binding properties of propamidine as compared to pentamidine [cf. Edwards, K. J., Jenkins, T. C., & Neidle, S. (1992) *Biochemistry 31*, 7104–7109]. This is seen to result from (i) decreased minor groove width at the binding site and (ii) reduced mobility of the bound propamidine molecule.

Propamidine, 1,3-bis(4-amidinophenoxy)propane, is a short-chain homologue of the drug pentamidine [1,5-bis(4-amidinophenoxy)pentane; NSC-620107] (Figure 1), which is active against the *Pneumocystis carinii* pathogen. Pentamidine has been extensively used for the treatment of *P. carinii* pneumonia (PCP), the opportunistic infection occurring in over 70% of AIDS patients (Montgomery et al., 1987; Gazzard et al., 1989; Golden et al., 1989; Wispelwey et al., 1991). The mechanism of pentamidine action against *P. carinii* is unknown but there is considerable evidence to suggest that direct interaction with the pathogenic genome is important (Jones et al., 1990; Tidwell et al., 1990). The X-ray crystal structure of pentamidine bound to the DNA sequence d(CGCGAATTCGCG)$_2$ has recently been determined in this laboratory (Edwards et al., 1992b) and shows binding of the pentamidine within the AT-rich region of the DNA minor groove. This behavior has recently been confirmed by NMR for binding to the dodecamer d(CGCAAATTTGCG)$_2$ in aqueous solution (Jenkins et al., 1993).

Associated with the use of pentamidine in the clinic are a number of toxic side effects. Several studies have been carried out to find improved linked bis(amidine) analogues with diminished toxicity and greater efficacy. This work has utilized DNA-binding affinities between DNA and these agents, as estimated from measurements of thermal denaturation (Tidwell et al., 1990; Cory, 1992; Cory et al., 1992; Fairley et al., 1993) and computer-assisted molecular modeling (Cory et al., 1992; Greenidge et al., 1993). These studies have demonstrated a significant correlation between the DNA-binding affinities of pentamidine analogues and their anti-PCP activity in a rat model (Cory et al., 1990; Tidwell et al., 1990).

Results from these studies have shown that propamidine has an increased DNA-binding affinity as compared to pentamidine, with a 40% increase in the thermal denaturation temperature (T_m) of the DNA–drug complex (Cory et al., 1992). Molecular modeling calculations predict propamidine binding to be more favorable than that of pentamidine, largely as a result of reduced perturbation of the DNA helix (Greenidge et al., 1993).

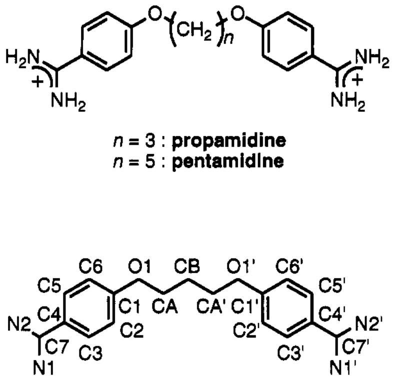

FIGURE 1: Structures of propamidine and pentamidine, together with the propamidine numbering scheme.

This paper reports the crystal structure of propamidine bound to the DNA sequence d(CGCGAATTCGCG)$_2$ and examines the structural features that are responsible for the differences in binding as compared to pentamidine.

MATERIALS AND METHODS.

Synthesis and Crystallization. The DNA dodecamer d(CGCGAATTCGCG) was purchased from the Oswel DNA Service (University of Edinburgh, Edinburgh, U.K.) and annealed before use. Propamidine was synthesized in this laboratory as the dihydrochloride salt.

The complex was grown as colorless needle-shaped crystals from sitting drops at 286 K. The best crystal was grown from a drop containing 4.5 mL of 47% (v/v) 2-methylpentane-2,4-diol (MPD), 2 mL of 15 mM propamidine, 4 mL of 100 mM MgCl$_2$, and 4 mL of 3 mM DNA equilibrated against a reservoir containing 1 mL of 40% MPD. All of the solutions were prepared using 30 mM sodium cacodylate buffer, pH 7.0, and were added together in the order listed to prevent drug precipitation. Crystals of X-ray quality were obtained after 1 week.

Data Collection. A crystal of approximate size 0.1 × 0.15 × 0.75 mm was mounted in a 0.5-mm Lindemann glass capillary with a small amount of mother liquor. Intensity

---

[†] This work is supported by the Cancer Research Campaign.

[‡] Final refined coordinates have been deposited in the Brookhaven Protein Data Bank under filename 1PRP.

[*] To whom correspondence should be addressed.

[®] Abstract published in *Advance ACS Abstracts,* November 15, 1993.

0006-2960/93/0432-13838$04.00/0

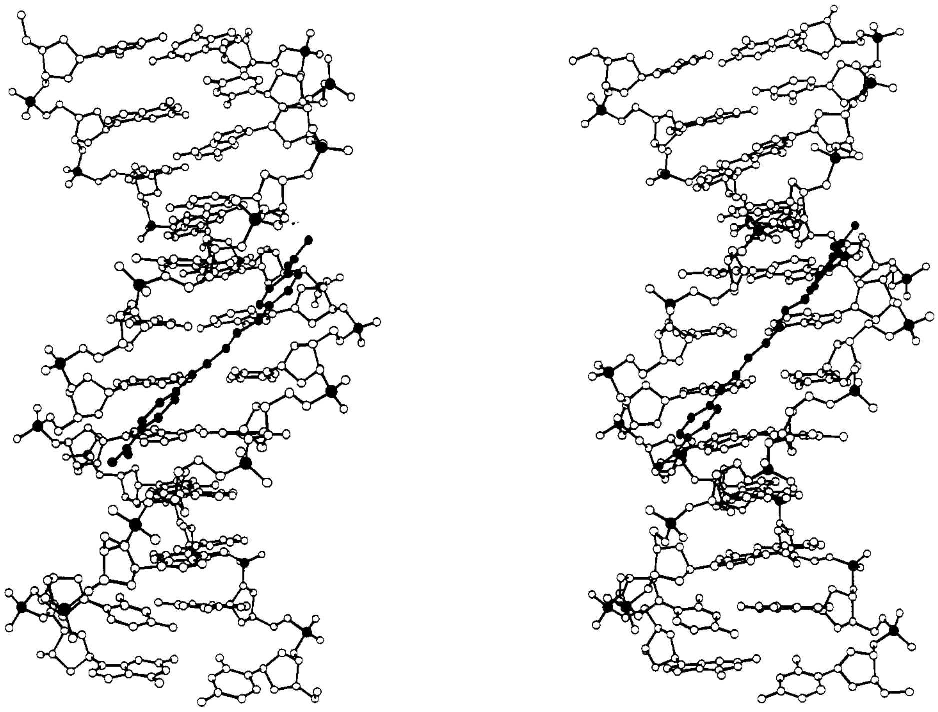

FIGURE 2: Views of (left) the propamidine–d(CGCGAATTCGCG)$_2$ complex and (right) the pentamidine–d(CGCGAATTCGCG)$_2$ complex, from Edwards et al. (1992b).

data were collected at 289 K using a Siemens-Xentronics multiwire area detector equipped with a rotating anode X-ray generator (40 mA, 70 kV) and graphite monochromator. A crystal-to-detector distance of 8 cm and swing angle of 12° were used to collect data to a resolution of 2.1 Å. The crystal data were collected with ϕ and χ set at 0° and 45°, respectively, while the crystal was rotated through 200° in ω; 180-s frames were recorded every 0.2° step. No crystal decay was observed during the data collection.

Data processing was carried out using the XENGEN (version 2.1) program package. A total of 11 478 of a possible 14 043 reflections were collected to a resolution of 2.1 Å. These data were then merged to give 4021 of the 4442 possible unique reflections (90.5%) with a merging R-value of 8.3%. A total of 2786 of these reflections were observed at the $2\sigma(F)$ level.

Structure Solution and Refinement. The unit cell dimensions of the crystal are $a = 25.00$, $b = 40.88$, and $c = 67.28$ Å, in the orthorhombic space group $P2_12_12_1$. This cell is close to that reported for the native dodecamer sequence (Dickerson & Drew, 1981), which has dimensions of $a = 24.87$, $b = 40.39$, and $c = 66.20$ Å, suggesting that the two structures are isomorphous. In light of this, the coordinate file for the native dodecamer sequence was obtained from the Nucleic Acid Database (Berman et al., 1992) and used as a starting model for the structure refinement. Initial refinement was carried out by constrained–restrained least-squares procedures using the program CORELS (Sussman, 1984). Rigid-body refinement of the DNA molecule as one constrained group was performed with the resolution range of the data used gradually increased from 10–4 Å (621 reflections) to 8–3 Å (1392 reflections). The R-value decreased to 35.3%. The molecule was then divided into 48 rigid groups comprising the 24 nucleosides, the 22 phosphate groups, and the two O5′ atoms at the 5′-terminus of each strand. The structure was refined by assigning rigid-body rotations and translations to each of the 48 groups. The resolution range was increased to a maximum value of 8–2.5 Å (2206 reflections) with the refinement converging to an R-value of 26.8%.

Refinement was continued using the program X-PLOR (Brünger, 1987). Forty cycles of conjugate-gradient energy minimization were carried out with all atomic temperature factors set at 25.0 Å^2 and using all data from 8–2.1 Å. This was followed by a run of simulated annealing for which the temperature was decreased from 1000 to 300 K in 25-K steps and molecular dynamics calculations carried out for 0.5 fs at each step. After the simulated annealing 120 cycles of conjugate-gradient energy minimization were performed. The R-factor at this stage was 23.7%. Electron density maps were calculated and displayed using the graphics package O, version 5.7 (Jones et al., 1991). The DNA molecule was well fitted within the density of the $2F_o - F_c$ map with a continuous lobe of density visible at this stage, lying in the minor groove of the DNA. The structure for a molecule of propamidine having an extended conformation was manually fitted into this density and refinement continued using conjugate-gradient positional refinement and atomic temperature factor refinement. Atom-centered potential charges for propamidine were calculated using the MNDO wave function (Orozco et al., 1990); additional force-field parameters were interpolated from molecular modeling studies carried out in this laboratory (Jenkins et al., 1993). The drug molecule was refitted and solvent positions were included in the refinement, being assigned as water molecules. At the end of the refinement a total of 73 water atoms were included to give a final R-value of 17.4%, for all data in the range 8–2.1 Å. The X-PLOR refinement and R-factor calculations used data with $F > 2\sigma$. Final refined coordinates, together with observed and calculated structure factors, have been deposited in the Brookhaven Protein Data Bank under filename 1PRP.

RESULTS

The crystal structure of the complex shows the propamidine molecule bound to the dodecamer duplex in the AT region of the minor groove. A view of the structure together with that of the analogous pentamidine complex (Edwards et al., 1992b) is shown in Figure 2. The propamidine lies at the center of the DNA duplex, with a number of hydrogen-bonding

Table I: Helical Parameters for the DNA Dodecamer

base pair	tip (°)	incline (°)	buckle (°)	propeller twist (°)	base step	roll (°)	twist (°)	slide (Å)	cup (°)
C1:G24	0	11	−7	−14	C1pG2	0	38	0.2	7
G2:C23	0	9	0	−10	G2pC3	−10	37	0.8	5
C3:G22	−10	7	5	−3	C3pG4	3	31	0.8	−11
G4:C21	−7	4	−6	−10	G4pA5	6	35	0.0	6
A5:T20	−1	1	1	−15	A5pA6	2	39	−0.2	0
A6:T19	1	0	0	−22	A6pT7	−3	30	−0.5	−2
T7:A18	−2	0	−2	−12	T7pT8	1	36	−0.1	5
T8:A17	−1	0	4	−14	T8pC9	0	39	0	−1
C9:G16	−1	−2	2	−8	C9pG10	5	32	0.9	−5
G10:C15	4	−3	−3	−5	G10pC11	−7	39	0.8	0
C11:G14	−3	−7	−3	−19	C11pG12	−4	38	0.3	−1
G12:C13	−7	−7	−5	17					

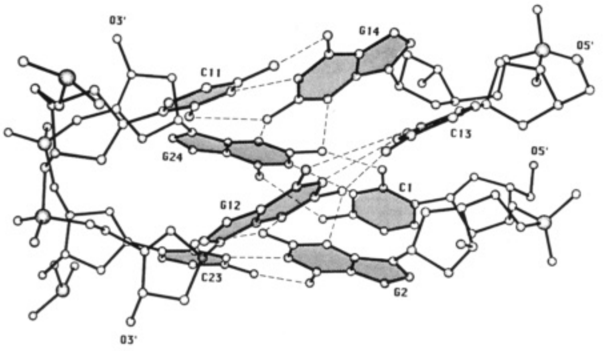

FIGURE 3: Base interactions for the terminal two residues of the d(CGCGAATTCGCG)$_2$ sequence, viewed approximately perpendicular to the base planes.

interactions between the terminal amidinium groups of the propamidine and the DNA.

DNA Structure. The DNA conformation observed in the complex is of B-type and is very similar to that seen previously for the native dodecamer sequence (Dickerson & Drew, 1981) and its drug-bound complexes [e.g., Brown et al. (1992) and Edwards et al. (1992b)]. The helical parameters computed for the DNA in the propamidine complex are shown in Table I. As was previously noted in the native sequence (Dickerson & Drew, 1981), the duplexes pack in the unit cell with the two terminal G·C base pairs at either end of the DNA interacting with the next DNA duplex via minor groove base–base interactions. In this arrangement a guanine of a guanine–cytosine Watson–Crick base pair in one duplex interacts with another screw axis-related guanine residue by means of a pair of N2···N3 hydrogen bonds. This (noncoplanar) three-center base-pairing is illustrated in Figures 3 and 4.

Features of the Bound Propamidine Molecule. The propamidine molecule in the complex has a twisted conformation as a consequence of its aromatic rings lying coplanar with the walls of the minor groove; the two rings are twisted by 30° with respect to one another. This compares with a 35° twist for the pentamidine molecule in the pentamidine–dodecamer structure (Edwards et al., 1992b). The terminal (four-atom) planes of the amidinium groups (C4–C7–N1–N2 and C4′–C7′–N1′–N2′) are twisted by 3° and 17°, respectively, from coplanarity with the phenyl rings to which each is bonded. The corresponding angles in the pentamidine complex are 3° and 6°. The central -CO(CH$_2$)$_3$OC- linkage of the propamidine molecule has torsion angles of (C1′–O1′–CA′–CB) −178°, (O1′–CA′–CB–CA) −170°, (CA′–CB–CA–O1) −166°, and (CB–CA–O1–C1) −171°. The oxygen···oxygen (O1···O1′) distance of 4.7 Å found here for propamidine compares with that of 7.1 Å in pentamidine, whereas the N1···N1′ distance of 14.6 Å in the latter is only 0.7 Å shorter than that observed in the pentamidine complex.

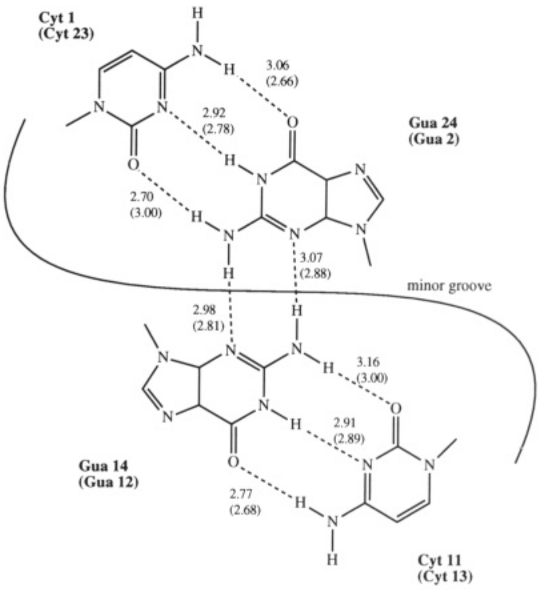

FIGURE 4: Schematic view of the base interactions for the propamidine–d(CGCGAATTCGCG)$_2$ complex.

DNA–Propamidine Interactions. Figure 5 shows the hydrogen-bonded interactions between the amidinium groups of the propamidine and the minor groove of the DNA dodecamer sequence. One end of the propamidine molecule interacts directly with atoms O2 of Cyt 9, N3 of Ade 17, and O4′ of Ade 18 and also with a water molecule. The other end interacts with O4′ and N3 of Ade 6 and both O4′ and O2 of Cyt 9. This latter contact with O2 is an indirect one, mediated through a water molecule. The pattern of contacts is generally very similar to that found in the crystal structure of the pentamidine complex (Edwards et al., 1992b), apart from the switch of hydrogen bonding involving N3 of Ade 5 in the pentamidine complex and N3 of Ade 6 in the present structure. The pentamidine and propamidine molecules are constrained to be in similar positions in this region of the DNA groove (due to the narrowed AT minor groove width), although the binding site size for the latter drug is shorter by ca. half a base pair separation (as indicated by the contact to Ade 6 rather than Ade 5, as well as the longer drug–DNA hydrogen bond distances). Figure 6 displays the interactions viewed along the minor groove for the propamidine–dodecamer complex.

The minor groove width of the DNA in the region of propamidine binding is shown in Figure 7, together with that found in the native structure (Dickerson & Drew, 1981) and the pentamidine complex (Edwards et al., 1992b). Both pentamidine and propamidine complexes show widened minor grooves as compared to the native dodecamer, which contains a spine of hydration along the AT region of the minor groove (Kopka et al., 1983). Within the region of ligand binding the

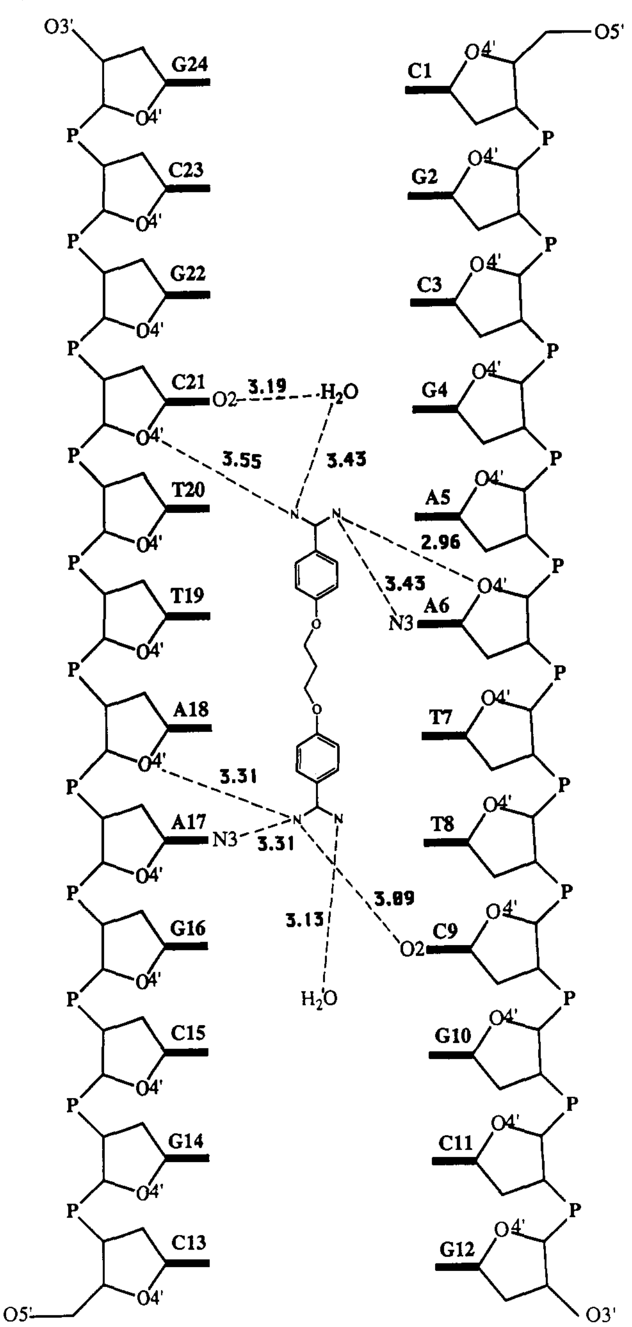

FIGURE 5: Schematic representation of the hydrogen-bonded interactions between the propamidine molecule and the d(CGCGAATTCGCG)$_2$ sequence. P represents -OPO(O$^-$)CH$_2$O-.

DNA minor groove is narrower for the propamidine complex, as compared with that found for the pentamidine-bound DNA, resulting in a width reduction of ~0.3 Å.

The phenyl rings and aliphatic chain of the propamidine molecule lie close to the floor and walls of the minor groove. Hydrogen atom positions for the propamidine and DNA atoms have been calculated, and the short contacts between the two molecules are shown in Table II. Both of the phenyl rings have an edge lying close to the floor of the groove. The methylene groups CA and CA′ are positioned close to the groove floor while CB is directed away from it.

Water Network. A network (external spine) of water molecules has been found to lie along the outer edge of the minor groove, extending along most of the propamidine molecule. These solvent molecules are shown in Figure 8 together with their local geometries. They are positioned at van der Waals or greater distance from the drug molecule. Propamidine linker chain atoms OA, CB, and OA′ face toward the water molecules, with the shortest propamidine···water contacts for these atoms being 5.2, 5.0, and 4.5 Å, respectively. Figure 9 shows the water molecules viewed from above the minor groove and toward the propamidine molecule. One of these waters lies close to the phosphate oxygen atom O2P of Cyt 21. The other water molecules in the spine are at rather longer separations to phosphate groups of residues Cyt 9, Gua 10, and Thy 20. Each of the water molecules observed over the mouth of the minor groove has one, two, or three neighboring waters, with separations ranging from 3.2 to 4.5 Å. In addition to this external spine hydration, a number of water molecules were found to be hydrogen-bonded to the phosphate groups and to bases lying in the major groove.

DISCUSSION

The DNA sequence d(CGCGAATTCGCG)$_2$ used in this structure has been studied extensively when complexed with noncovalent minor groove ligands [e.g., Kopka et al. (1985), Coll et al. (1987), Brown et al. (1990), and Lane et al. (1991)]. In addition, a number of native dodecamer sequences of the type d(CGN$_8$CG)$_2$, where the central eight base-pair tract is AT-rich, have been examined using X-ray crystallography and NMR techniques [e.g., Yoon et al. (1988), Lane et al. (1991), Larsen et al. (1991), Edwards et al. (1992a), and Jenkins et al. (1993)]. All of these dodecamer sequences crystallize in the orthorhombic space group $P2_12_12_1$ and are isomorphous. In these structures the base interactions that exist between the terminal two C·G base pairs of neighboring duplexes upon packing of the unit cells serve to stabilize the structures. This results in an AT-rich template at the center of the dodecamer sequence that is free from crystal packing influences, to which ligands can bind. The minor groove three-center G·G·C base-pairing arrangement is notable in itself, suggesting that third-strand DNA recognition can occur in the minor as well as the more conventional major groove, when the former is sufficiently wide.

Propamidine is bound to the AT-rich minor groove of the dodecamer and lies centrally positioned within the groove. The symmetric placement of the ligand found in the crystal structure is unlikely to result from crystal packing effects but contrasts to the NMR solution structure of this complex (T. C. Jenkins and A. N. Lane, unpublished results), in which the propamidine is displaced from the center of the DNA by a half base pair along the helix axis. This asymmetric binding behavior in solution is in accord with other NMR studies of AT-rich oligonucleotide duplexes with both symmetric and nonsymmetric bis(amidine) ligands (Brown et al., 1990; Lane et al., 1991; Jenkins et al., 1993). The reasons for such binding site differences between the X-ray and NMR results are not fully understood, although it must be borne in mind that the two sets of experiments are performed under very different conditions of ionic strength and alcohol concentration, both of which can significantly affect DNA conformation.

The positively-charged propamidine interacts with the dodecamer directly via hydrogen bonding to the bases and sugar groups which line the surface of the minor groove, and also by van der Waals contacts with the floor and walls of the groove. Hydrogen-bonded interactions occur from the amidinium groups of Ade 6, Cyt 9, and Ade 17 as well as to the sugar O4′ atoms of residues Ade 6, Ade 18, and Cyt 21. These interactions thus extend from the N3 atom of base Ade 6 to the N3 atom of Ade 17. The propamidine binding within the AT tract of the DNA is thus approximately half a base pair shorter than the corresponding binding site for pentamidine,

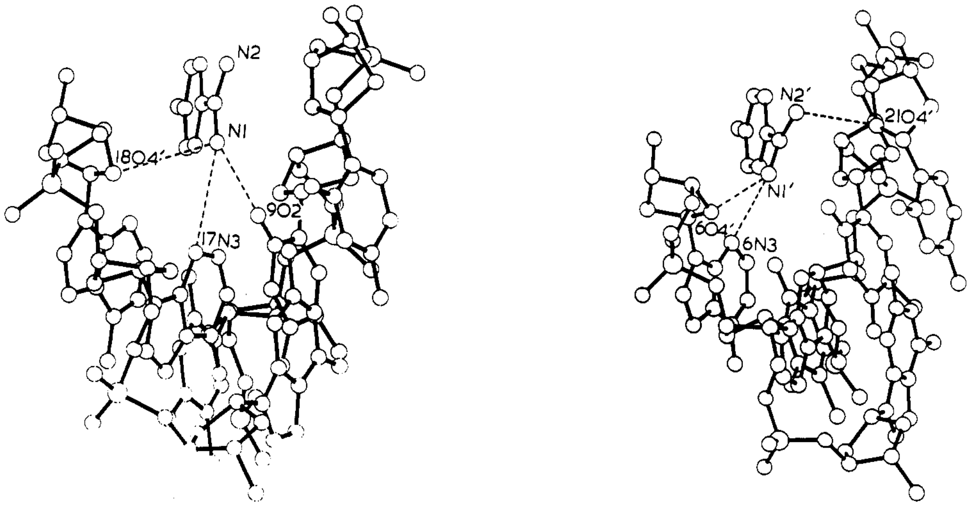

FIGURE 6: Propamidine–DNA minor groove hydrogen-bonded interactions.

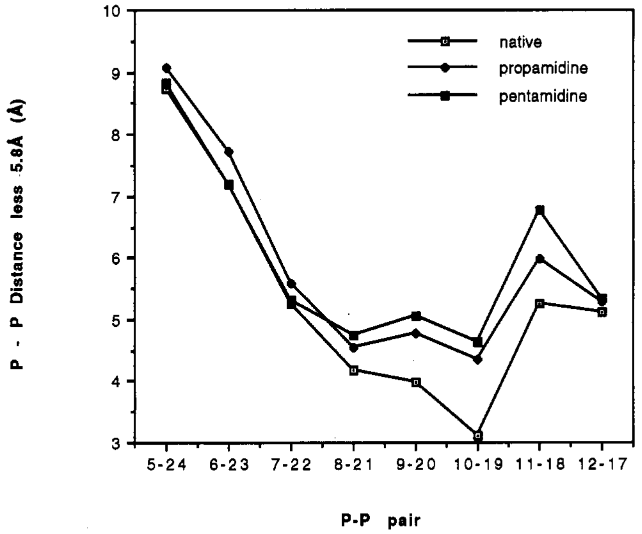

FIGURE 7: Plot of DNA minor groove width for the native dodecamer, propamidine–bound dodecamer, and pentamidine-bound dodecamer sequences.

Table II: Close Contacts between Propamidine and DNA (<2.9 Å)

propamidine atom	DNA atom	distance (Å)
phenyl H		
H2–C2	18H2	1.9
	18C2	2.6
	18N3	2.5
H3–C3	17H2	2.0
	17C2	2.8
	8O2	2.8
H2′–C2′	6H2	2.0
	6C2	2.8
H3′–C3′	20O2	2.5
	6H2	2.4
	6C2	2.6
phenyl C		
C2′	6H2	2.7
C3′	20O2	2.7
aliphatic H		
HA1–CA	8O4′	2.7
HA2–CA	19O2	2.3
HB1–CB	8C4′	2.8
HA1′–CB	20O4′	2.7
	19O2	2.8
HA2′–CA′	7O2	2.8

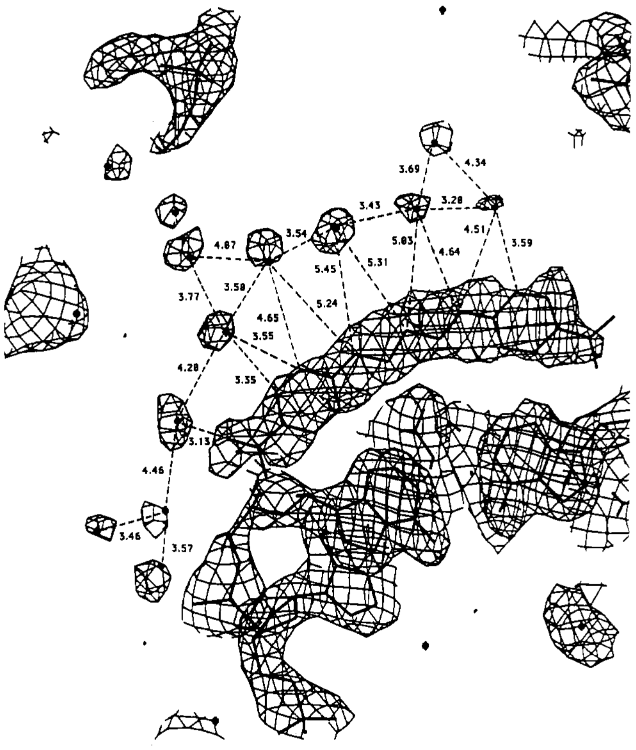

FIGURE 8: $2F_o - F_c$ map (1σ level) of the propamidine molecule and water molecules within the DNA minor groove.

where there is more extended interaction with atom N3 of bases Ade 5 and Ade 17. The apparent shorter length of propamidine as compared to pentamidine (ca. 2.5 Å in the fully extended conformation), which is less than the mean DNA helical rise of 3.4 Å, is actually only 0.7 Å in terms of the N1⋯N1′ distances, which are the critical ones for base recognition. The fact that this difference is a small one is in part a result of the differences in the deviations from pure staggered conformations that result from twisting of the drugs around the minor groove and in part from the enhanced twist of the amidinium groups in propamidine. Thus the propamidine molecule effectively spans less than half a base pair less than pentamidine.

The aliphatic chain and phenyl groups of the propamidine molecule contact the floor of the minor groove via residues Ade 6, Thy 7, Thy 8, Ade 17, Ade 18, Thy 19, and Thy 20; by comparison, pentamidine makes a number of additional contacts, to residues Ade 5 and Cyt 21.

Hydration of the Complex. An interesting feature of this structure is the novel role of the water molecules. The spine of hydration which occurs deep within the minor groove of the

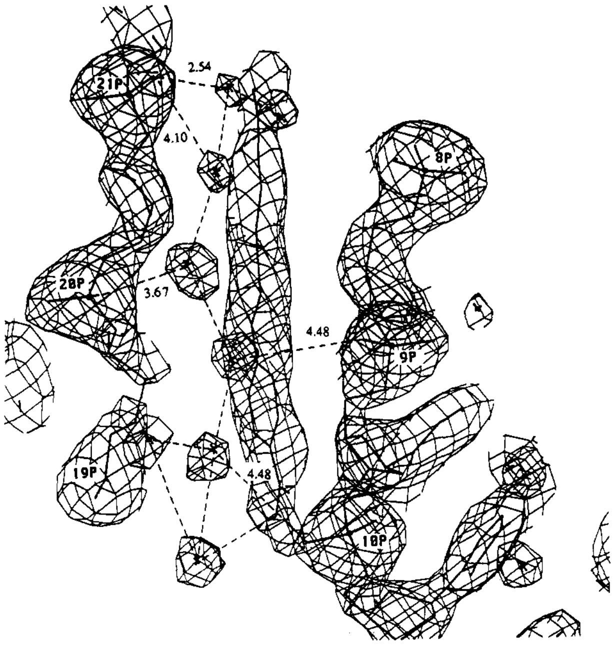

FIGURE 9: $2F_o - F_c$ map of the external spine of water molecules surrounding the mouth of the minor groove, viewed looking toward the propamidine molecule.

native dodecamer sequence has been displaced by propamidine binding. Instead we find a continuous spine of solvent molecules, lying along the outer edge of the minor groove. To our knowledge, this is the first report of such a water spine; a similar feature was not seen for the pentamidine complex. It is notable that three of these water positions lie close to (<0.5 Å) water positions observed in the native dodecamer structure (Kopka et al., 1983).

The solvent positions are noncoplanar and unsymmetrically positioned across the width of the groove. The water···water separations range from 3.2 to 4.5 Å and are longer than the expected O···O hydrogen-bonding distance seen for water molecules (Chiari et al., 1982). Distances in excess of 4.1 Å for DNA to water interactions have been shown to occur in the crystal structure of the dodecamer sequence d(CGCGAATT^{Br}CGCG)$_2$ (Kopka et al., 1983), accounting for almost a third of all hydrogen-bond distances seen within the major groove of the DNA and 50% of those bound to the terminal O3′ and O5′ atoms. A more recent study of DNA base hydration (Schneider et al., 1992), examined distances up to 4 Å from base atoms involved in direct hydration with the DNA bases. For the propamidine–DNA complex we consider that at least some of the water positions along the outer edge of the groove may be involved in direct hydration with the complex. This hydrophobic cluster of molecules is analogous to, but much more extensive than, the hydrophobic shell observed around the methyl groups of thymine bases (Schneider et al., 1992).

DNA Binding Affinity. We observe a narrower DNA minor groove width in this structure at the propamidine binding site as compared with that seen for pentamidine. This reduction indicates that the DNA groove has closed up more tightly to bind the propamidine molecule, in accord with the observation that propamidine is more tightly bound than pentamidine (Cory et al., 1992; Greenidge et al., 1993). The atomic thermal parameters of the pentamidine molecule in the crystal structure of pentamidine bound to DNA range from 54 to 67 Å^2 (Edwards et al., 1992b). This compares to values of 33–44 Å^2 for propamidine in the present study. High atomic thermal parameters were not shown to occur in the associated DNA molecule for the pentamidine-bound complex and thus may result from high atomic motion of the weakly associated ligand. Lower mobility for the ligand in the propamidine–dodecamer complex would thus be a consequence of its superior binding affinity.

REFERENCES

Berman, H. M., Olson, W. K., Beveridge, D. L., Westbrook, J., Gelbin, A., Demeny, T., Hsieh, S., Srinivasan, A. R., & Schneider, B. (1992) *Biophys. J. 63*, 751–759.

Brown, D. G., Sanderson, M. R., Skelly, J. V., Jenkins, T. C., Brown, T., Garman, E., Stuart, D. I., & Neidle, S. (1990) *EMBO J. 9*, 1329–1334.

Brünger, A. T., Kuriyan, J., & Karplus, M. (1987) *Science 235*, 458–460.

Chiari, G., & Ferraris, G. (1982) *Acta Crystallogr. B38*, 2331–2341.

Coll, M., Frederick, C. A., Wang, A. H.-J., & Rich, A. (1987) *Proc. Natl. Acad. Sci. U.S.A. 84*, 8385–8389.

Cory, M. (1992) *Med. Chem. Res. 1*, 417–424.

Cory, M., Tidwell, R. R., & Fairley, T. A. (1992) *J. Med. Chem. 35*, 431–438.

Dickerson, R. E., & Drew, H. R. (1981) *J. Mol. Biol. 151*, 761–768.

Edwards, K. J., Brown, D. G., Spink, N., Skelly, J. V., & Neidle, S. (1992a) *J. Mol. Biol. 226*, 1161–1173.

Edwards, K. J., Jenkins, T. C., & Neidle, S. (1992b) *Biochemistry 31*, 7104–7109.

Fairley, T. A., Tidwell, R. R., Donker, I., Naiman, N. A., Ohemeng, K. A., Lombardy, R. J., Bentley, J. A., & Cory, M. (1993) *J. Med. Chem. 36*, 1746–1753.

Gazzard, B. G. (1989) *J. Antimicrob. Chemother. 23*, 67–75.

Golden, J. A., Chernoff, D., Hollander, H., Feigal, D., & Conte, J. E. (1989) *Lancet i*, 654–657.

Greenidge, P. A., Jenkins, T. C., & Neidle, S. (1993) *Mol. Pharmacol. 43*, 982–988.

Jenkins, T. C., Lane, A. N., Neidle, S., & Brown, D. G. (1993) *Eur. J. Biochem. 213*, 1175–1184.

Jones, S. K., Hall, J. E., Allen, M. A., Morrison, S. D., Ohemeng, K. A., Reddy, V. V., Geratz, J. D., & Tidwell, R. R. (1990) *Antimicrob. Agents Chermother. 34*, 1026–1030.

Jones, T. A., Zou, J.-Y., Cowan, S. W., & Kjeldgaard, M. (1991) *Acta Crystallogr. A47*, 110–119.

Kopka, M. L., Fratini, A. V., Drew, H. R., & Dickerson, R. E. (1983) *J. Mol. Biol. 163*, 129–146.

Kopka, M. L., Yoon, C., Goodsell, D., Pjura, P., & Dickerson, R. E. (1985) *Proc. Natl. Acad. Sci. U.S.A. 82*, 1376–1380.

Lane, A. N., Jenkins, T. C., Brown, T., & Neidle, S. (1991) *Biochemistry 30*, 1372–1385.

Larsen, T. A., Kopka, M. L., & Dickerson, R. E. (1991) *Biochemistry 30*, 4443–4449.

Montgomery, A. B., Luce, J. M., Turner, J., Lin, E. T., Debs, R. J., Corkery, K. J., Brunette, E. N., & Hopewell, P. C. (1987) *Lancet ii*, 480–482.

Schneider, B., Cohen, D., & Berman, H. M. (1992) *Biopolymers 32*, 725–750.

Sussman, J. L. (1984) in *Methods and Applications in Crystallographic Computing* (Hall, S. R., & Ashida, T., Eds.) pp 206–237, Clarendon Press, Oxford, U.K.

Tidwell, R. R., Jones, S. K., Geratz, J. D., Ohemeng, K. A., Cory, M., & Hall, J. E. (1990) *J. Med. Chem. 33*, 1252–1257.

Wispelwey, B., & Pearson, R. D. (1991) *Infect. Control Hosp. Epidemiol. 12*, 375–381.

Yoon, C., Privé, G. G., Goodsell, D. S., & Dickerson, R. E. (1988) *Proc. Natl. Acad. Sci. U.S.A. 85*, 6332–6336.